INSTITUTE OF PHYSICS PUBLISHING NANOTECHNOLOGY
Nanotechnology **18** (2007) 044017 (5pp) doi:10.1088/0957-4484/18/4/044017

Nanoplasmonic enhancement of single-molecule fluorescence

Palash Bharadwaj, Pascal Anger and Lukas Novotny

The Institute of Optics and Department of Physics and Astronomy, University of Rochester, Rochester, NY 14627, USA

E-mail: novotny@optics.rochester.edu

Received 18 August 2006
Published 12 December 2006
Online at stacks.iop.org/Nano/18/044017

Abstract

We demonstrate that the fluorescence rate from a single molecule with near-unity quantum yield can be enhanced by a factor of ≈10 by use of a single laser-irradiated noble metal nanoparticle. The increased fluorescence rate is primarily the result of the local field enhancement. However, at particle–molecule distances shorter than 2 nm, nonradiative decay of the excited molecule due to energy transfer to the metal dominates over the local field enhancement giving rise to fluorescence quenching. These counteracting processes depend on the wavelength-dependent dielectric function of the particle antenna. In this study, we quantitatively compare single-molecule fluorescence enhancement near 80 nm gold and silver nanoparticles excited at a fixed wavelength of $\lambda = 637$ nm. In accordance with theory we find similar enhancements for both gold and silver nanoparticles.

(Some figures in this article are in colour only in the electronic version)

1. Introduction

Despite the ever-increasing trend towards miniaturization, the detection and manipulation of light on length scales smaller than 100 nm remains a challenging endeavour. New vistas towards the realization of this goal have been opened up through the development of near-field optical microscopy in the last two decades [1]. Early approaches made use of tiny apertures for confining optical fields beyond the limits of diffraction [1–4] and more recently it was realized that subwavelength light confinement can also be established with laser-irradiated metal tips [5]. The external irradiation gives rise to a strongly localized and enhanced field at the tip apex which is then used as a secondary light source for the excitation of a local spectroscopic response (fluorescence, Raman scattering, absorption, etc) of a sample placed close by [6, 7]. A high-resolution optical map of the sample surface is recorded by raster-scanning the tip over the sample surface and recording a spectroscopic signature point by point. It was soon realized that laser-irradiated metal tips are the optical analogues of electromagnetic antennas widely employed in the radiowave and microwave regimes [5]. Basically, the job of an antenna is to convert the energy associated with free propagating radiation (laser) into localized energy (near-field) centred on the receiver (sample). This analogy puts near-field optical microscopy into a new perspective, and the term 'optical antenna' is becoming common in scientific parlance [8].

An antenna is a reciprocal device, mediating between a source (or detector) and free radiation. At optical frequencies, the most fundamental source (or detector) is an elementary two-level quantum system. A single fluorescent molecule with a small Stokes shift and near-unity quantum yield comes close to the ideal two-level atom, and thus captures the essence of photophysical processes that take place in more complex systems. Studying the interaction between an optical antenna and a single molecule is, therefore, of both scientific and technological interest.

An optical antenna enhances the local field and, therefore, when placed near a single molecule, increases the molecule's excitation rate [9, 10]. The latter is directly proportional to the molecule's fluorescence rate as long as the antenna does not affect the molecule's quantum yield. In this case, the fluorescence enhancement due to the presence of the optical antenna is a direct measure of the antenna gain. Unfortunately, the antenna does affect the quantum yield. When placed next to an excited molecule, it introduces nonradiative decay channels

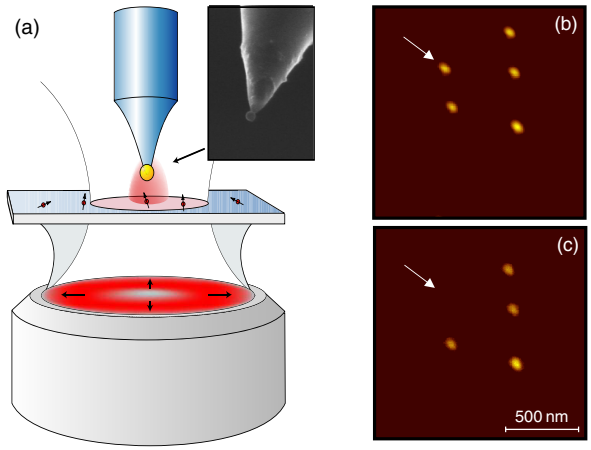

Figure 1. (a) Schematic diagram of the experimental setup. A radially polarized laser beam is focused on the surface of a glass coverslip with well-separated single dye molecules. The fluorescence is monitored as a function of the proximity of a single gold or silver nanoparticle antenna attached to the end of a glass tip. The inset shows an SEM image of a nanoparticle tip. (b) Topographic image of a sample with isolated gold particles before picking and (c) after picking.

and thereby lowers the fluorescence rate. At very close separations between antenna and molecule, the nonradiative energy transfer becomes so strong that the fluorescence of the molecule becomes quenched [9–11]. This fluorescence quenching is not merely of pathological interest, as it is likely to be present in any realistic application where optical energy transduction takes place, but it puts a practical upper bound on the maximum signal gain that can be achieved with an optical antenna.

In order to understand antenna-coupled light absorption and emission we studied optical antennas in the form of a noble metal colloid. The simple spherical geometry makes a quantitative comparison between theory and experiment possible. A single fluorescent molecule was used as both a receiver and a transmitter. We monitored the fluorescence yield of the molecule as a function of the antenna's position and its composition (gold and silver). Spherical gold and silver particles have plasmon resonances at the wavelengths of 530 and 355 nm, respectively, which render them useful for antenna applications in the visible spectrum. Previous studies predicted that the fluorescence enhancement is maximized not at the plasmon resonance wavelength, but rather at a wavelength red-shifted from it [9, 12]. For this reason, we chose to work at a wavelength of 637 nm, which is red-shifted from the resonance peaks of both gold and silver particles. For our experiments we used Nile Blue molecules because of their high intrinsic quantum yield and small Stokes shift (absorption and emission peaks at 631 and 661 nm, respectively). Single gold and silver nanoparticles were attached to the end of a sharply etched glass fibre which, in turn, was mounted to a quartz tuning fork. The latter provides a shear-force feedback signal used to control the distance between particle and sample [13]. A schematic diagram of the experimental setup is shown in figure 1(a). In our experiments we selected individual Nile Blue molecules and measured their fluorescence yield as a function of the vertical position of the metal particle. We used this approach to quantitatively compare the fluorescence enhancement efficiencies of gold and silver particles.

2. Experimental methods

Single metal nanoparticle were attached to the end of a glass tip following the recipe in [14]. Briefly, short pieces of an optical glass fibre were first etched in 49% HF to generate sharp tips with end diameters of ∼50 nm. The etched fibres were cleaned with piranha solution overnight before further treatment with 5% 3-aminopropyltriethoxysilane (APTES) in acetone for 5 h. Commercial gold and silver colloids (80 nm in diameter) were spun on a clean coverslip treated with a 10:90 mixture of 1 M NaOH and ethanol to give a coverage of ∼0.1 particles μm^{-2}. A functionalized glass tip was attached onto a quartz tuning fork for use as a regular tip on a shear-force-based scanning probe microscopy (SPM) platform. The glass tip was then positioned over a single Au or Ag particle and slowly approached towards the sample until the particle firmly attached to the tip (cf figures 1(b), (c)). This technique relies on electrostatic interactions between the functionalized-glass surface and the negatively charged colloid particle, and hence works for both Au and Ag particles. An SEM micrograph of a typical tip thus fabricated is shown in the inset of figure 1.

Both near- and far-field single molecule fluorescence measurements were performed with a confocal setup based on an inverted microscope. A 637 nm radially polarized laser beam was focused with a high numerical aperture (NA) microscope objective on the surface of a transparent glass cover slip with well-separated Nile Blue molecules. The radial polarization ensures a strong longitudinal field (along the optical axis) in the laser focus. Single molecule samples were prepared by spin-casting a 10 μl drop of 1 nM Nile Blue on a cleaned coverslip. To reduce photobleaching and to orient the molecules in different directions each sample was overcoated by a thin layer (2–4 nm) of (poly)methylmethacrylate (PMMA), also by spin-coating. The fluorescence from single molecules was detected while the sample was raster-scanned in the focal plane. The emission from single molecules was first spectrally filtered with a set of bandpass filters and then detected using a single photon counting module. Near-field fluorescence images were recorded by placing a single gold or silver particle in the focus of the exciting laser beam and keeping it at a constant height (∼5 nm) from the sample surface by means of shear-force feedback [16, 15].

3. Results and discussion

To characterize the antenna efficiency of a single nanoparticle we first recorded confocal and near-field fluorescence images of the single molecule sample using a particle–sample separation of ≈5 nm. Characteristic fluorescence rate images are shown in figure 2. The near-field image was recorded with a 80 nm silver particle, but similar results are also obtained with gold particles of the same size. Both gold and silver nanoparticles gave rise to a strong fluorescence enhancement resulting in a vastly improved spatial resolution over the confocal image. The near-field image of a single molecule renders a characteristic pattern which originates from

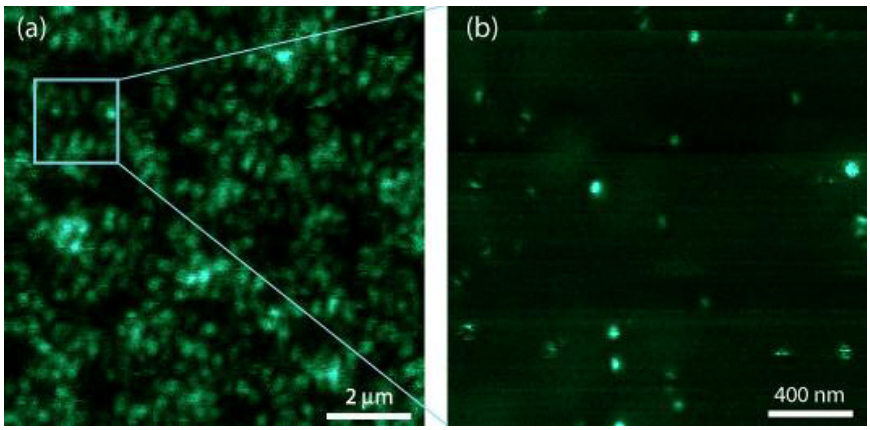

Figure 2. Fluorescence rate images of single molecules recorded by raster-scanning a sample of Nile Blue relative to a stationary laser focus ($\lambda = 637$ nm). (a) 10 μm $\times$ 10 μm confocal scan yielding a resolution of $\approx$250 nm. (b) 2 μm $\times$ 2 μm near-field scan of the marked region using an 80 nm silver particle as an optical antenna placed into the laser focus at a height of 5 nm above the sample surface. A resolution to 65 nm is deduced from the near-field images.

the particular orientation of the molecule's absorption dipole moment [17]. Because of the radially polarized excitation beam and the axial symmetry of the antenna, vertically oriented molecules (dipole axis perpendicular to sample surface) render circular fluorescence spots while horizontally oriented molecules appear as a two-lobe pattern. In this case, the molecular dipole moment is parallel to the line interconnecting the two lobes. Molecules that are not perfectly horizontal show also up as a two-lobe pattern but with one lobe brighter than the other [17]. As expected, the enhancement for vertically oriented molecules was greater than that for molecules lying horizontal or at an angle.

In order to quantitatively compare the fluorescence enhancement due to gold and silver particles we selected a single vertically oriented molecule and recorded the fluorescence rate as a function of the particle–sample separation. In addition to the fluorescence originating from the molecule we also recorded weak fluorescence from the glass cover slip as well as luminescence from the gold or silver particle. To correct for this background, we placed the particle on an empty region of the sample surface and recorded the distance dependence of the detected photon rate (data not shown). This count rate was then subtracted from the previously measured fluorescence curve of a single molecule to yield the net fluorescence approach curve. Figure 3 shows corrected fluorescence rate curves for both gold and silver particles.

We note that for both silver and gold particles, fluorescence quenching dominates over the enhancement of the excitation rate at very short distances, leading to a drop in the overall fluorescence rate [9, 11]. The maximum fluorescence enhancement, defined as the ratio of the maximum near-field fluorescence and the net far-field fluorescence, can be readily estimated from the traces shown in figure 3. The enhancement for the gold particle is approximately nine-fold, only slightly weaker than the enhancement for the silver particle.

To understand the similar enhancement of gold and silver particles we have performed a theoretical study in which the fluorescence yield is modelled as a two-step process according to [9]:

$$\gamma_{\mathrm{em}}(\mathbf{r}, \omega) = \gamma_{\mathrm{exc}}(\mathbf{r}, \omega) q(\mathbf{r}, \omega). \quad (1)$$

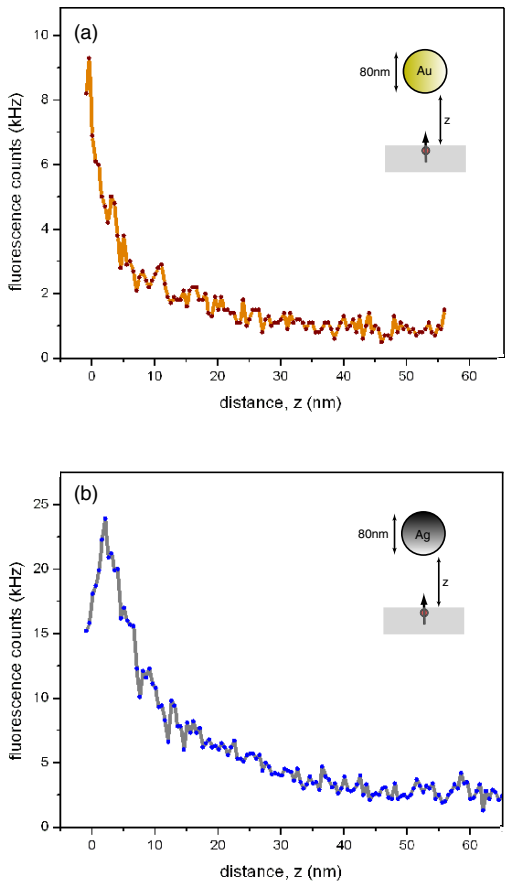

Figure 3. Single molecule fluorescence rate as a function of particle–sample distance for (a) an 80 nm gold particle and (b) an 80 nm silver particle. At short distance the fluorescence enhancement drops due to nonradiative decay (energy transfer from the excited molecule to the particle). Both gold and silver particles yield similar enhancement at the excitation wavelength of $\lambda = 637$ nm.

Here, γ_{em} is the fluorescence emission rate, γ_{exc} is the excitation rate, and q is the quantum yield. The latter can be expressed in terms of the radiative decay rate γ_{r} and the

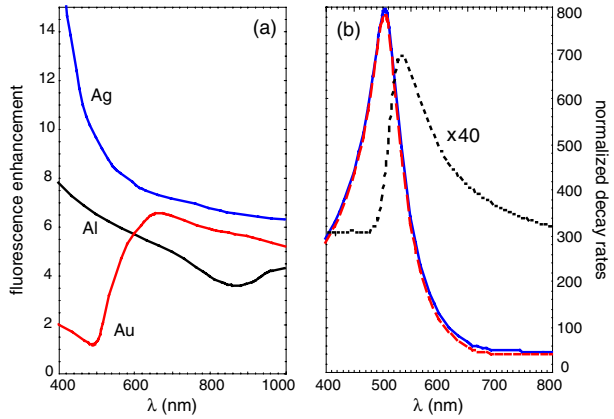

Figure 4. Calculated fluorescence enhancement and decay rates. (a) Fluorescence enhancement as a function of the excitation wavelength λ evaluated at a distance of 5 nm from metal particles (80 nm diameter) made of gold, silver, and aluminium. At $\lambda = 637$ nm the enhancements for gold and silver particles are nearly the same. (b) Spectral dependence of the decay rates evaluated at a distance of 5 nm from a gold particle. The radiative decay rate (dotted curve) peaks to the red of the plasmon resonance whereas the nonradiative decay rate (dashed curve) and the total decay rate (solid curve) coincide with the plasmon peak.

nonradiative decay rate γ_{nr} of the excited molecule as $q = \gamma_r/[\gamma_r + \gamma_{nr}]$. Close to the metal particle both rates can be enhanced. They can be described in terms of the system's dyadic Green's function and hence by treating the molecule as a simple dipole emitter [18]. The two-step process represented in equation (1) is justified because vibrational relaxation destroys the quantum coherence between the excitation and emission process. Also, far from saturation, the excitation rate can be expressed as $\gamma_{exc} \propto |\mathbf{p} \cdot \mathbf{E}(\mathbf{r}, \omega)|^2$, with $\mathbf{E}$ being the local (enhanced) electric field and $\mathbf{p}$ being the absorption dipole moment.

For simplicity, we ignored the presence of the dielectric surface and considered a single molecule at a distance of 5 nm from the surface of a 80 nm particle made of gold, silver or aluminium. We calculated the enhancement of the fluorescence rate as a function of the excitation wavelength according to equation (1) and used experimentally determined dielectric functions [19, 20]. The results of our calculations are summarized in figure 4(a). At $\lambda = 637$ nm, the calculated fluorescence enhancement factors for gold and silver particles are in the range of 7–8, which is in good agreement with our experiments. Slight deviations originate from the simplified model, which ignores the dielectric interface, from the experimental variation of the thickness of the PMMA layer, and from the orientational uncertainty of the molecules. For $\lambda = 637$ nm our calculations predict a lower fluorescence enhancement for aluminium particles. However, at shorter wavelengths the enhancement for silver and aluminium particles becomes very strong. Fluorescence enhancement in excess of 100 is calculated for silver particles excited at $\lambda = 360$ nm and for aluminium particles excited at $\lambda = 200$ nm. Interestingly, the largest enhancements are found at frequencies red-shifted from the surface plasmon resonance frequency of the particles. This finding has its origin in the different spectral behaviour of the radiative and nonradiative decay rates, as shown in figure 4(b) for the case of an 80 nm gold particle. The nonradiative decay rate (γ_{nr}) coincides with the plasmon frequency but then drops rapidly towards the red. On the other hand, the radiative decay rate (γ_r) peaks towards the red side of the plasmon resonance and hence the quantum yield q becomes larger for wavelengths red-detuned from the plasmon resonance. However, at the same time, the excitation rate (γ_{exc}) becomes weaker with increasing wavelength and, combined with the trend of the quantum yield, gives rise to a maximum of the fluorescence yield to the red of the plasmon peak. Notice that the radiative rate is much smaller than the nonradiative rate, indicating that at a distance of 5 nm the molecule mostly relaxes nonradiatively through energy transfer to the particle.

4. Conclusions

In conclusion, we have studied and compared the efficiency of spherical gold and silver nanoparticles acting as optical antennas for single molecule fluorescence enhancement. We found that the maximum fluorescence enhancement induced by gold and silver particles are comparable. Our results are in agreement with theoretical predictions and are of importance for the development of novel biodetection schemes providing single-molecule sensitivity at a high throughput.

Acknowledgments

This research was funded by the National Science Foundation through grant ECS-0210752 and the US Department of Energy through grant DE-FG02-01ER15204. We are grateful to Shanlin Pan and Lewis Rothberg for help with surface chemistry.

References

[1] Pohl D W, Denk W and Lanz M 1984 *Appl. Phys. Lett.* **44** 651–3
[2] Lewis A, Isaacson M, Harootunian A and Muray A 1984 *Ultramicroscopy* **13** 227–31
[3] Fischer U Ch 1985 *J. Vac. Sci. Technol.* B **3** 386
[4] Betzig E, Trautman J K, Harris T D, Weiner J S and Kostelar R L 1991 *Science* **251** 1468–70
[5] Novotny L and Stranick S J 2006 *Ann. Rev. Phys. Chem.* **57** 303–31
[6] Hartschuh A, Beversluis M R, Bouhelier A and Novotny L 2004 *Phil. Trans. R. Soc.* A **362** 807–19
[7] Keilmann F and Hillenbrand R 2004 *Phil. Trans. R. Soc.* A **362** 787–97
[8] Muehlschlegel P, Eisler H-J, Martin O J F, Hecht B and Pohl D W 2005 *Science* **308** 1607–9
[9] Anger P, Bharadwaj P and Novotny L 2006 *Phys. Rev. Lett.* **96** 113002
[10] Kühn S, Hakanson U, Rogobete L and Sandoghdar V 2006 *Phys. Rev. Lett.* **97** 017402
[11] Frey H G, Witt S, Felderer K and Guckenberger R 2004 *Phys. Rev. Lett.* **93** 200801
[12] Thomas M, Greffet J J and Carminati R 2004 *Appl. Phys. Lett.* **85** 3863
[13] Karrai K and Grober R D 1995 *Appl. Phys. Lett.* **66** 1842–4
[14] Kalkbrenner T, Ramstein M, Mlynek J and Sandoghdar V 2001 *J. Microsc.* **202** 72–5
[15] Toledo-Crow R, Yang P C, Chen Y and Vaez-Iravani M 1992 *Appl. Phys. Lett.* **60** 2957–9

[16] Betzig E, Finn P L and Weiner S J 1992 *Appl. Phys. Lett.* **60** 2484–6
[17] Novotny L, Beversluis M R, Youngworth K S and Brown T G 2001 *Phys. Rev. Lett.* **86** 5251–4
[18] Xu Y, Lee R K and Yariv A 2000 *Phys. Rev.* A **61** 33807
[19] Johnson P B and Christy R W 1972 *Phys. Rev.* B **6** 4370–9
[20] Smith D Y, Shiles E and Inokuti M 1985 *Handbook of Optical Constants of Solids* ed E D Palik (New York: Academic) p 369